ELSEVIER

Journal of Nuclear Materials 258–263 (1998) 1060–1065

journal of nuclear materials

Investigation on modification of plasma facing surface under long duration discharges by means of a collector probe in TRIAM-1M

Takeshi Hirai [a,*], Kazutoshi Tokunaga [b], Tadashi Fujiwara [b], Naoaki Yoshida [b], Satoshi Itoh [b], the TRIAM group [b]

[a] *Interdisciplinary Graduate School of Engineering Sciences, Research Institute for Applied Mech., Kyuhsu University, Ksuga, Fukuoka 816-8580, Japan*

[b] *Research Institute for Applied Mechanics, Kyuhsu University, Ksuga, Fukuoka 816-8580, Japan*

Abstract

Metallic specimens mounted on a collector probe head were inserted in the scrape-off layer and exposed to long pulse tokamak plasma in TRIAM-1M. Strong radiation damage (formation of interstitial loops) was caused by high energy (>2 keV) charge-exchange hydrogen neutrals. The surfaces of the probe specimens were covered by new material made of co-deposited in-vessel elements such as Fe, Cr, Mo, O and C. The deposited layer was often exfoliated by blistering. These results indicate that energetic hydrogen neutrals and the co-deposition of impurities considerably change the surface properties of plasma facing components and even introduce new impurity sources.

1. Introduction

In magnetically confined hot plasma devices, sputtering erosion of plasma facing materials and the behavior of the sputtered atoms from the plasma and redeposition have been studied extensively at large tokamak devices such as TEXTOR [1], ASDEX-Upgrade [2], JET [3,4] and JT-60U [5], because the behavior of impurity atoms and modification of plasma facing surface layers directly affect plasma confinement. As pointed out by Behrisch et al. [4] the composition and structure of the final surface layers are different from those of the materials initially installed, because the surface layers of the vessel walls are modified by the plasma due to erosion, redeposition, hydrogen isotope implantation and heating. On the other hand, it was reported that the tokamak plasma caused remarkable displacement damage in the surface layers and may result in degradation of the materials [6,7].

The surface modifications mentioned above are the integrated effects of plasma-wall interaction, and therefore very long exposure to plasma is required to stabilize the phenomena. In most of the experiments in the present tokamaks, the test samples are exposed to hundreds of discharges; nevertheless the plasma performance is different from shot to shot. In order to study the phenomenon effectively and quantitatively, long pulse discharge operation is very helpful. In this sense, the superconducting tokamak TRIAM-1M at Kyushu University, in which hot plasma can be sustained for more than 2 h by lower hybrid current drive [8], is very suitable for such purposes. In the present work, therefore, collector probe experiments were carried out at TRIAM-1M by exposure to one or several ultra long pulse discharges in order to study the modification of surface layers by plasma wall interaction.

2. Experimental procedure

TRIAM-1M is a high field tokamak with Nb_3Sn superconducting toroidal field magnets. Its major and

* Corresponding author. Tel.: +81-92 583 7719; fax: +81-92 583 7690; e-mail: hirai@riam.kyushu-u.ac.jp.

0022-3115/98/$19.00
PII: S0022-3115(98)00278-5

minor radii are 0.8 m and 0.115 m × 0.175 m, respectively. Three poloidal ring limiters, made of Mo, were used for protection of the vacuum vessel made of 304SS. The last closed flux surface (LCFS) was determined by the limiter which protruded 17 mm from the inner wall of the vacuum vessel.

Al, Cu and W were used as probe specimens. Disk specimens with a diameter of 3 mm were annealed in a high vacuum and thinned by electro-polishing for transmission electron microscopy (TEM) observation. The specimens mounted on the plasma facing side (P-side) and the electron drift side (E-side) of the collector probe head were introduced into the vacuum vessel of TRIAM-1M through a horizontal port by using a ultra-high vacuum sample transfer system [6].

Two plasma exposure experiments named Probe #1 and Probe #2 were carried out in hydrogen plasma. The specimens of Probe #1 were exposed for 78.4 min. (5 successive discharges with 18 kW of a lower current drive discharge (LHCD) input power, $I_P = 20$ kA, $n_e = 2\text{–}3 \times 10^{12}$ cm^{-3}. $T_i = 0.6$ keV). The specimens on the P-side were located just at the inner wall level of the vacuum vessel (17 mm outside the LCFS) and those on the E-side were located in the shadow of inner wall (1.7 mm outside the wall) as shown in Fig. 1(a). The specimens of Probe #2 were exposed to an ultra-long discharge for 72.3 min with 10 kW of LHCD input power ($I_P = 18$ kA). The specimens in the P-side were located in the scrape-off layer (at 10 mm from the inner wall level or 7 mm outside the LCFS). Those on the E-side also were located in the scrape-off layer as illustrated in Fig. 1(b). The temperature of the specimens during exposure was not measured for lack of a temperature monitoring system.

After exposure, microstructural and microchemical changes in the specimens were examined by means of TEM, Auger electron spectrometry (AES) and energy dispersive spectrometry (EDS).

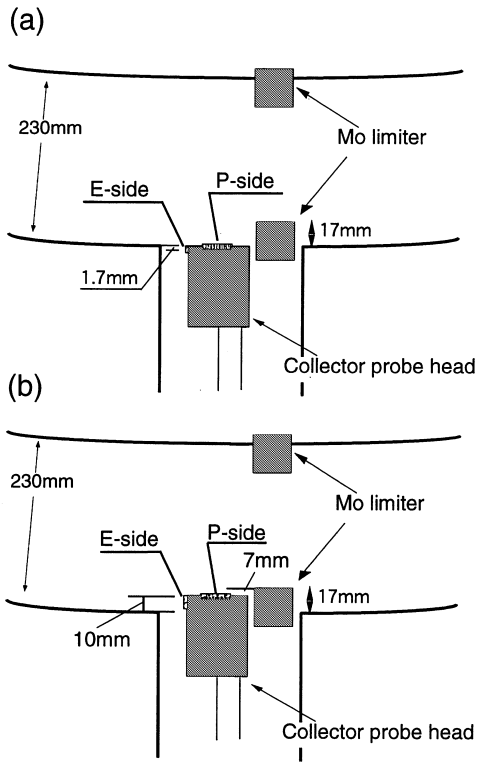

Fig. 1. Schematic view of the collector probe experiments: (a) Probe #1 and (b) Probe #2. The collector probe head was introduced horizontally.

3. Results

3.1. Probe #1 experiment

Fig. 2 shows bright field images and the corresponding electron diffraction patterns for the specimens placed on the P-side at the wall surface level and on the E-side in the shadow of plasma. A large number of radiation induced dislocation loops with black dot contrast or loop contrast were formed in all specimens except for the Al irrespective of their position. It is notable that dislocation loops were formed even in W which requires high energy incident particles for the formation of radiation induced dislocation loops.

Orange-peel-like unusual images were observed particularly in Al and Cu specimens placed on the P-side. These specimens gave diffuse diffraction rings in addition to their diffraction spots. Fig. 3(a) shows dark field images obtained from a part of the diffraction rings (circled in the diffraction pattern) of a Cu specimen on the P-side. With this imaging condition, crystalline grains satisfying the Bragg diffraction condition, have white contrast. These results show that the probe specimens are covered by nanocrystalline material with an average grain size of about 1 nm.

AES analysis with Ar sputtering was carried out for the Al specimen placed at the P-side to determine the chemical composition of the deposited material. AES spectra for several sputtering times and for different depths are shown in Fig. 4. In addition to O and C, metallic elements such as Fe, Cr and Mo, which are components of the vacuum vessel (304SS) and Mo from the limiters, were detected. The concentrations of the metallic elements Mo, Fe, Cr and Ni analyzed by EDS were 42, 39, 16 and 3 at.%, respectively. The thickness of the deposited layer estimated by TEM technique [9] was approximately 15 nm. This implies that the average fluxes of metallic impurities onto the inner wall were 8.6×10^{16}, 1.2×10^{17} and 4.2×10^{16} atoms/m^{2}s for Mo, Fe and Cr, respectively. This result corresponds well qualitatively with the previous results [6,7].

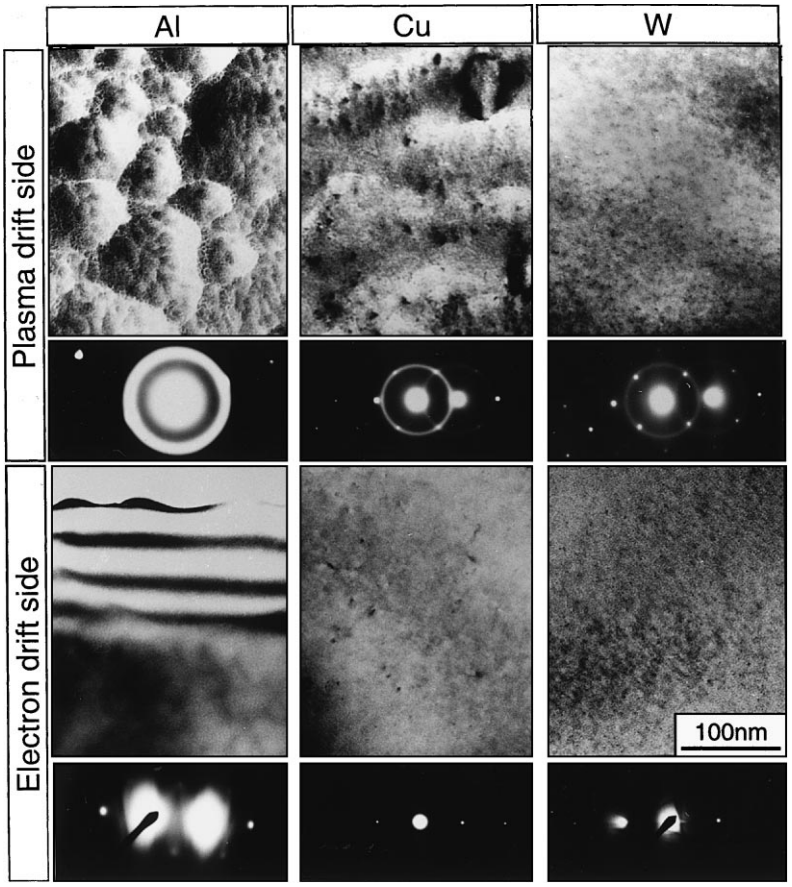

Fig. 2. Bright field images and electron diffraction patterns obtained from the specimens at the P-side and the E-side in Probe #1.

Fig. 5 shows bright field image of Al on the P-side at low magnification. The figure shows that the impurity layers deposited in Al are exfoliated by forming blisters. This result indicates that gas atoms, probably hydrogen implanted together with metallic impurities, cause blistering by accumulating at the interface between the Al substrate and the deposited impurity layer.

The orange-peel-like images and diffraction rings were not observed in any specimens placed at the E-side.

3.2. Probe #2 experiment

Fig. 6 shows bright field TEM images and electron diffraction patterns obtained from the W specimens placed at the P-side (a) and the E-side (b) in the scrape-off layer. In both cases, interstitial-type dislocation loops were formed. The Depthe distribution of the dislocation loops from the P-side is plotted in Fig. 7 together with damage distributions of the defects corresponds well with those for energetic ions higher than a few keV.

Electron diffraction rings in Fig. 6(b) indicate that an impurity layer is formed on the probe specimen at the E-side. AES analysis showed that major metallic impurity is Mo in this case. Fig. 3(b) shows a diffraction pattern and a dark field image obtained from a part of diffraction ring of W specimen placed at the E-side. These data shows that the impurity layer is bcc polycrystalline material with an average grain size of about 20 nm. One can note that the properties of the deposited materials are different from those of the Probe #1 experiment and the previous results [6,7].

No clear diffraction rings were observed for the specimens placed at the P-side though they were in the scrape-off layer. AES analysis also showed the surface composition of metallic impurities was less than the detection limit. These result indicate that sputtering is superior to impurity deposition.

4. Discussion

4.1. Radiation damage by neutral particles.

In general, interstitials and vacancies are formed in crystalline materials, if the knock-on energy exceeds the displacement threshold energy (E_d). Interstitial, which

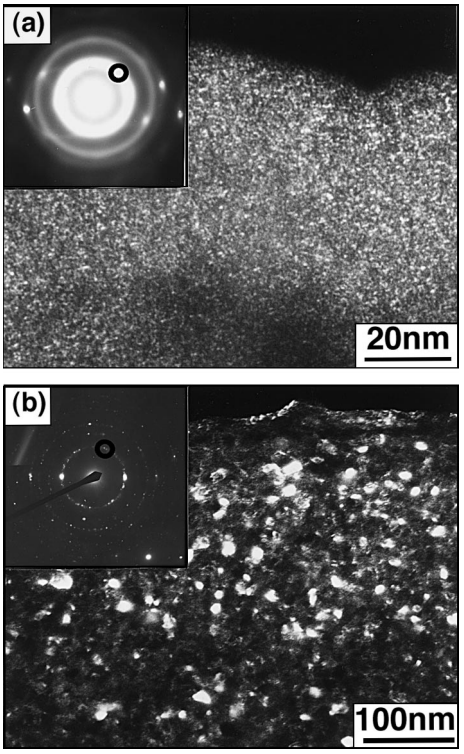

Fig. 3. Electron diffraction patterns and dark field images obtained from a part of diffraction ring marked in the figure. (a) Cu specimen at the P-side in Probe #1, (b) W specimen at the E-side in Probe #2. White contrast in dark field images shows individual grains satisfying the Bragg condition.

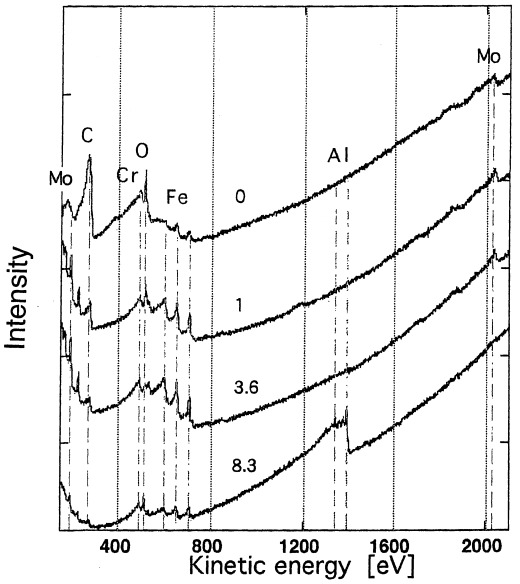

Fig. 4. AES of an Al specimen at the P-side in Probe #1. The peaks of deposited materials appeared until Al substrate. The numbers in figure show the relative sputtered depth. The deposited material was analyzed with the Al substrate detected at a depth of 8.3.

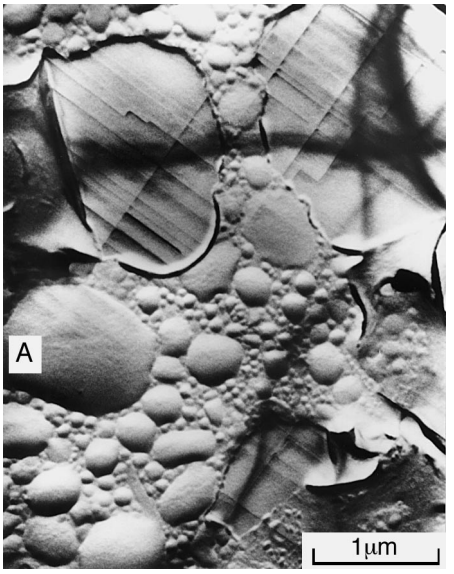

Fig. 5. Low magnification Bright field images in Al specimen at the P-side in Probe #1. Blistering and flaking of the deposited layer were observed.

are highly mobile in most metals above room temperature, migrate freely and form clusters. It is expected that the dislocation loops observed in the many probe specimens are formed in such process. The maximum knock-on energy T is given by

$$T = \frac{4M_1M_2}{(M_1 + M_2)^2}E,$$

where E is the energy of bombarding particles, M_1 and M_2 are the weight mass of the incident particle and the target atom, respectively. We can consider that the bombarding particles which created dislocation loops would be hydrogen atoms, because the narrow damage range of impurity atoms such as O and Mo are not consistent with the wide distribution of dislocation loops as shown in Fig. 7. Since E_d for W is 44 eV [10], the energy of the bombarding hydrogen particles required for the formation of the displacement damage is estimated to be more than 2050 eV. This was confirmed by hydrogen ion irradiation experiments [11]. These facts indicate that fairly large numbers of hydrogen particles with energy more than 2 keV existed in the plasma of TRIAM-1M sustained by LHCD, though the ion temperature was about 500 eV.

The specimen placed at the E-side in Probe #1 was in the shadow of inner wall where plasma particles moving

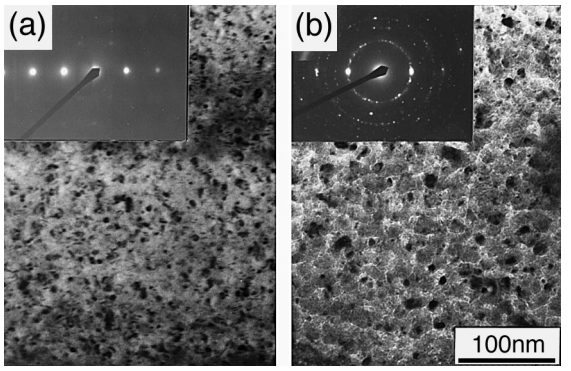

Fig. 6. Bright field images and electron diffraction patterns obtained from the specimens at the P-side (a) and the E-side (b) in Probe #2.

along magnetic field could not reach. Even if gyration motion at the edge plasma were taken into account, radiation damage at that position (1.7 mm standing back from inner wall) cannot be explained. As partly discussed in the previous works [6,7], the dislocation loops were formed by bombardment of neutral particles but not by the ionized particles. We should note that charge exchanged neutral particles play important roles in the radiation damage of plasma facing materials.

The temperature of the probe specimen was not monitored directly during plasma exposure but it must increase due to heat load from the plasma and thermal radiation from the nearby Mo limiter. The temperature increase in the specimen is expected to be the reason for finding no defect formation in Al, in which formation of interstitial loops in Cu as shown in Fig. 2 also suggests that an increase in temperature occurred during a long discharge.

4.2. Impurity deposition

The composition of deposited materials in Probe #1 and Probe #2 were different. Mo, Fe, Cr are co-deposited in the Probe #1 experiments but only Mo was found for the Probe #2 experiment. One possible explanation is that the vacuum vessel surface is covered by a Mo layer for the Probe #2 experiment, because a lot of high power discharge experiments were performed before the Probe #2 experiment, during which large amounts of Mo were evaporated from the Mo limiter and the Mo divertor due to the strong heat load.

In the case of the Probe #1 experiment, fcc nanocrystalline material was formed by the co-deposition of Mo, Fe, Cr, O and H, even though the simple alloys of the metallic elements have bcc structure. Similar phenomena were reported by Yoshida et al. [12] for co-deposited films of Fe and O that formed fcc nanocrystalline material depending on the content of O.

Blistering and flaking of the deposited impurity layers was observed for an Al specimen placed at the P-side

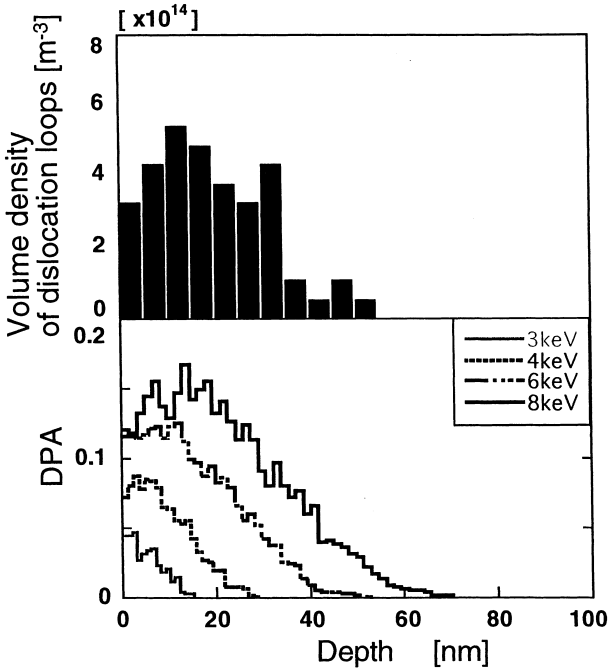

Fig. 7. Depth distribution of dislocation loops in W at the E-side in Probe #2 (top) and damage distributions estimated from the TRIM-code for various energies (bottom).

of Probe #1. It seems that implanted or co-deposited hydrogen atoms aggregate at the interface between the deposited layer and the substrate Al and form blisters if the inner gas pressure exceeds the critical value. Exfoliation of the impurity layer deposited on the top inner surface of the vacuum vessel may provide another impurity source. For instance, the blister marked "A" in Fig. 5 will produce about 1×10^9 impurity atoms. In fact, flashings in the plasma were often observed during long pulse discharges. The exfoliated impurity layer dropping into the plasma is a possible mechanism for the plasma flashing. This discussion is supported by the fact that much fine metallic dust was observed at the bottom of the vacuum chamber.

Present results indicate that co-deposition of several different elements may result in drastic changes for the properties of plasma facing surface. One should pay more attention on these surface modification in order to estimate the retention and recycling of tritium and the behavior of impurities.

5. Summary

Metallic specimens mounted on a collector probe head were exposed to the long pulse tokamak plasma of TRIAM-1M to determine the effects of plasma surface interactions on the surface properties of the plasma facing materials. In the case of the Probe #1 experiment, the collector probe head was placed at the position of the surface of the vacuum vessel and in the case of the Probe #2 it was in the scrape-off layer. In both cases, strong radiation damage in the form of interstitial loop occurred. Formation of defects in W located in the shadow of plasma flux indicates high energy (>2 keV) charge-exchange of hydrogen neutrals and heavy damage to plasma facing materials. The plasma facing surface was covered by a fcc nanocrystalline layer consisting of elements of the in-vessel materials such as Fe, Cr (vacuum vessel), Mo(limmiter and divertor), and O and C. The deposited material was often flaked due to blistering. In the case of the Probe #2 experiment, the plasma facing surface was covered by a polycrystalline Mo deposited layer. These results indicate that bombardment of high energy hydrogen neutrals and the co-deposition of impurities may considerably change the surface properties of plasma facing components and introduce new impurity sources.

References

[1] The TEXTOR team and the ALT-1 group, J. Nucl. Mater. 145–147 (1987) 3.
[2] J. Roth, D. Naujoks, K. Krieger, A. Field, G. Lieder, S. Hirsch, J. Nucl. Mater. 220–222 (1995) 231.
[3] R. Behrisch, A.P. Martinelli, S. Grigull, R. Groetzschel, U. Kreissig, D. Hhildebrant, W. Schneider, J. Nucl. Mater. 220–222 (1995) 590.
[4] R. Behrisch, M. Mayer, C. Garcia-Rosales, J. Nucl. Mater. 233–237 (1996) 673.
[5] H. Kudo, M. Shimada, T. Sugie, N. Hosogane, K. Itami, S. Tsujii, H. Nakamura, N. Asakura, A. Sakasai, Y. Kawano and the JT-60 Team, J. Nucl. Mater. 196–198 (1992) 71.
[6] N. Yoshida, A. Nagao, K. Tokunaga, K. Tawara, T. Muroga, T. Fujiwara, S. Itoh and the TRIAM Group, Radiation Effects and Defects in Solids 124 (1992) 99.
[7] K. Tokunaga, T. Muroga, T. Fujiwara, K. Tawara, N. Yoshida, S. Itoh and the TRIAM Group, J. Nucl. Mater. 191–194 (1992) 449.
[8] S. Itoh, K. Nakamura, M. Sakamoto, K. Makino, E. Jotaki, S. Kawasaki, H. Nakashima, T. Yamagajo, Proceedings of the 16th IAEA Fusion Energy Conference, Montreal, IAEA-CN-64/EP-6, 1996.
[9] D.B. Williams, C.B. Carter, Transmission Electron Microscopy, Plenum, New York, 1996, p. 369.
[10] L.K. Merkle, Radiation Damage in Metals, in: N.L. Peterson, D. Harkness (Eds.), American Society of Metals, Ohio, 1975, pp. 58–94.
[11] R. Sakamoto, T. Muroga, N. Yoshida, J. Nucl. Mater. 220–222 (1995) 819.
[12] N. Yoshida, F.E. Fujita, J. Phys. F: Metal Phys. 2 (1972) 1009.